26 May 2010, 4:45 pm - 6:45 pm

Dynamic Properties of Sand in Constant-Volume and Constant-Load Tests

F. Jafarzadeh
Sharif University of Technology, Iran

H. Sadeghi
Sharif University of Technology, Iran

Fifth International Conference on
Recent Advances in Geotechnical Earthquake Engineering and Soil Dynamics
and Symposium in Honor of Professor I.M. Idriss
May 24-29, 2010 • San Diego, California

DYNAMIC PROPERTIES OF SAND IN CONSTANT-VOLUME AND CONSTANT-LOAD TESTS

Jafarzadeh, F.
Sharif University of Technology
Tehran, Iran 11365-9313

Sadeghi, H.
Sharif University of Technology
Tehran, Iran 11365-9313

ABSTRACT

Constant-volume and constant-load tests were performed on Babolsar and Toyoura sands by using a modified SGI cyclic simple shear device which provides the capability of back pressure saturation. All tests were shear strain controlled and conducted under different values of relative density, vertical effective stress and shear strain amplitude. Results revealed that D_r, σ'_v and γ affect shear modulus and damping ratio under both constant-volume and constant-load conditions in similar ways except the shear strain amplitude which has no important influence on damping of constant-volume tests. The effects of D_r, σ'_v, γ and the number of cycles on variations of shear modulus and damping ratio of sand were found to be more pronounced under constant-load condition. It seems that the differences between the results may be due to the different fabric produced in two kinds of test samples rather than to the test method. However, further study is needed to clarify this issue.

INTRODUCTION

Wide application of dynamic properties of soil in geotechnical earthquake engineering problems (such as the analysis of soil-structure interactions, dynamic bearing capacity of machines foundations, soil structures subjected to cyclic loadings) has made researchers to investigate a variety of factors which affect shear modulus and damping ratio of soil (e.g. Hardin and Drnevich 1972a) and to develop various field and laboratory tests methods so far (Kramer 1996). A cyclic simple shear test is a convenient laboratory test method in evaluating G and D of soil, especially at large shear strains.

Results of truly undrained and conventional constant-volume tests by using a developed NGI direct simple shear device were compared by Dyvik et al. 1987. On the basis of static tests on clay, they concluded that the results obtained by two methods are equivalent for saturated soils. Theoretically, since there is no real pore pressure generation in the specimen under constant-volume condition, it is not necessary to saturate the specimen. However, poor saturation can modify soil resistance (Vanden Berghe et al. 2001).

The main objective of the present study is to investigate shear modulus and damping ratio of cyclically loaded sand under constant-volume and constant-load conditions. Additionally, the effects of some parameters on dynamic properties of sand under mentioned conditions will be presented and discussed.

LABORATORY PROCEDURE

Test Materials

Two poorly graded sands, Babolsar and the Japanese standard Toyoura sand were selected as test materials. The former is natural sand obtained from the South coast of Caspian Sea. Particle size distribution curves of sands are shown in Fig. 1.

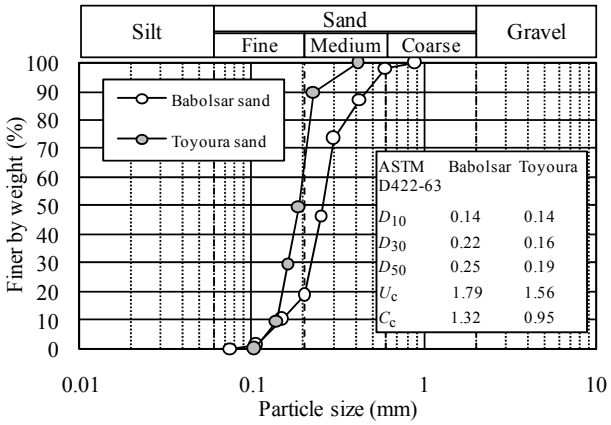

Fig. 1. Gradation curves of test materials.

Principal index tests were performed following the procedure of the ASTM standards. The physical properties of soils utilized in the all conducted tests are summarized in Table 1.

Table 1. Physical properties of test materials

Soil type	Specific gravity	e_{max}	e_{min}
Babolsar sand	2.753	0.777	0.549
Toyoura sand	2.645	0.973	0.609
Standard designation	ASTM D854–02	ASTM D4254–00	ASTM D4253–00

Apparatus

A servo-controlled pneumatic SGI cyclic simple shear, CSS; apparatus manufactured by Wykeham Farrance Co. was used in order to perform the cyclic loading of soil samples. This apparatus is capable of conducting stress and strain controlled tests in the both horizontal and vertical directions. Loading forces are applied through the pneumatic actuators mounted horizontally and vertically. A circular specimen is mounted between the base pedestal and piston top cap and surrounded by a number of circular rings to prevent lateral displacement during consolidation or shearing stages. Indeed, the specimen can be laterally restrained by rigid boundary plates (Cambridge-type device), a wire-reinforced membrane (NGI-type device), or a series of stacked rings (SGI-type device) according to the description of Kramer 1996.

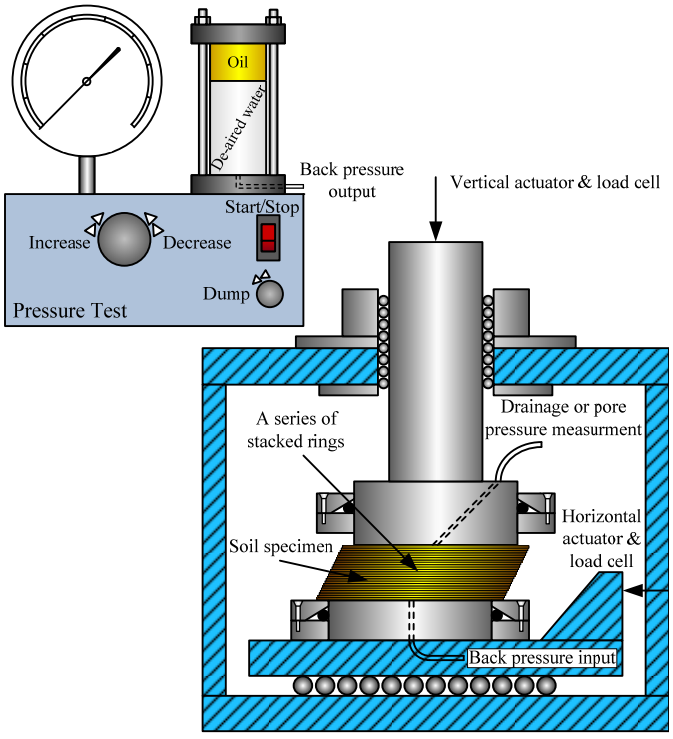

Fig. 2. Schematic view of cyclic simple shear (SGI type) apparatus and pressure test device.

The apparatus was equipped with a pressure test device made by ELE. The pressure test device which can introduce water pressure into the specimen was utilized in order to improve the apparatus so that it can be used in conducting undrained tests on fully saturated samples. On the other hand, the capability of saturating the specimen with back pressure has been possible using this ancillary device. A schematic illustration of the modified CSS apparatus is given in Fig. 2.

Sample Preparation

Constant-Volume Tests. Solid cylindrical samples with the nominal diameter of 70 mm and height of 22 mm were used in cyclic simple shear tests. Samples were prepared by using the moist placement method suggested by Ishihara 1996. The mixture of soil with 5% water content was poured in the mold with a spoon and the specimen was compacted until approaching the desired density. The relative density of the specimen was controlled by adjusting its height using a 0.01 mm digital caliper. This method of sample preparation was utilized in constant-volume and constant-load tests.

Estimation of Pore Pressure Parameter. Use of Skempton's pore pressure parameter, B value; in triaxial loading condition as a guide to achieve full saturation is conventional but, for the stress conditions other than triaxial condition e.g. where the specimen is consolidated under K_0 condition (Fig. 3a), there is no criteria for assuring full saturation of the sample. It seems that a proper evaluation of pore pressure parameter under this special loading condition is inevitable. Figure 3a shows a saturated soil element subjected to an increase of total stress in which the intermediate and minor principal stresses are equal. The pore water pressure will grow by Δu if drainage is not allowed from the soil. The change in the volume of pore water due to the increase of pore pressure by an amount of Δu can be expressed as (Das 1983):

$$\Delta V_p = nV_0C_p\Delta u \quad (1)$$

where n is porosity, V_0 is the original volume of soil element and C_p is the compressibility of pore water.

On the other hand, the change in volume of the soil skeleton due to the effective stress increment indicated in Fig. 3b will be:

$$\Delta V = C_cV_0(\Delta\sigma'_1 + \Delta\sigma'_2 + \Delta\sigma'_3) = C_cV_0(\Delta\sigma'_1 + 2\Delta\sigma'_2) \quad (2a)$$

where $\Delta\sigma'_1$, $\Delta\sigma'_2$ and $\Delta\sigma'_3$ are principal effective stresses as shown in Fig. 3b corresponding to the total stresses in Fig. 3a and C_c is the compressibility of the soil skeleton. Figure 3c shows the determination of C_c from laboratory compression test results under uniaxial stress application with zero excess pore water pressure. By simplifying Equation 2a, we obtain:

$$\Delta V = C_cV_0(\Delta\sigma'_1 + 2K_0\Delta\sigma'_1) = C_cV_0\Delta\sigma'_1(1 + 2K_0) \quad (2b)$$

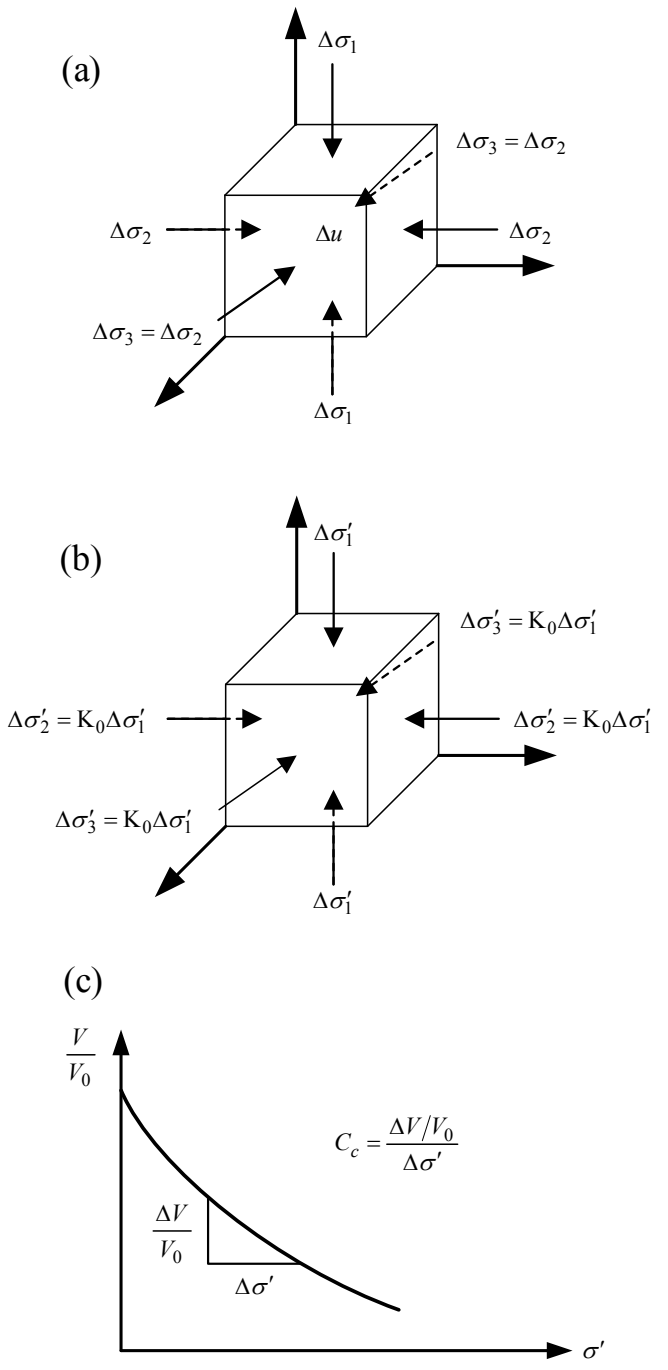

Fig. 3. (a) Total stresses and (b) Effective stresses imposed on a saturated soil element consolidated under K_0 *condition and (c) Definition of compressibility of soil skeleton (Das 1983).*

where K_0 is the coefficient of at–rest earth pressure. After substitute of $\Delta\sigma_1 - \Delta u$ for $\Delta\sigma'_1$ in Equation 2b we have:

$$\Delta V = C_c V_0(\Delta\sigma_1 - \Delta u)(1 + 2K_0) \quad (2c)$$

If the soil element is fully saturated with water, the change in the volume of both pore water and soil skeleton under the application of three principal total stresses plotted in Fig. 3a must be equal. So, a comparison of Equations 1 and 2c gives:

$$nV_0 C_p \Delta u = C_c V_0(\Delta\sigma_1 - \Delta u)(1 + 2K_0) \quad (3)$$

The pore pressure parameter, $\Delta u/\Delta\sigma_1$, is extracted from Equation 3 as:

$$\Delta u/\Delta\sigma_1 = (1 + 2K_0)/\left[nC_p/C_c + (1 + 2K_0)\right] \quad (4a)$$

Finally, by more simplification of Equation 4a, the pore pressure parameter can be estimated based on Equation 4b:

$$\Delta u/\Delta\sigma_1 = 1/\left[1 + nC_p/[C_c(1 + 2K_0)]\right] \quad (4b)$$

Since the compressibility of water is much smaller than compressibility of soil skeleton, the value of C_p/C_c converges to zero. So it would appear that, the value of $\Delta u/\Delta\sigma_1$ mainly depends on C_p/C_c than $n/(1+2K_0)$. Hence, the effect of K_0 value on the estimation of pore pressure parameter can be neglected. However, the value of $n/(1+2K_0)$ is less than unity and makes the term, $nC_p/[C_c(1+2K_0)]$ to decrease more. Subsequently, it can be inferred from the above expressions that, the upper limit of pore pressure parameter where the specimen is consolidated under the application of K_0 condition, is equal to one.

Traditionally, the value of pore pressure parameter under triaxial stress conditions, B value, equals to 0.95 is accepted as representing virtually full saturation in laboratory reports. As an alternative, if several successive equal increments of confining pressure give identical values of B, full saturation of the specimen could be assured (Head 1998).

Constant-Load Tests. After preparation of samples on the basis of wet tamping method, CO_2 was percolated through the specimens and de-aired water was then introduced into the soil sample, while the vertical stress was kept at 15 kPa to prevent the sample disturbance. After one stage of saturation using 25 kPa of vertical stress and 15 kPa of back pressure was taken, back pressure was raised following the vertical stress increase to the next step by 10 kPa and the procedure of raising the vertical stress and back pressure was then repeated. Considering the mentioned criteria for assuring full saturation, the saturation of the specimens by the application of back pressure was continued until two or three equal increments of vertical stress give identical values of pore pressure parameter, $\Delta u/\Delta\sigma_1$. The samples were then consolidated to a given vertical consolidation stress. The values of total vertical stress, effective consolidation stress and back pressure as well as the corresponding ratio of pore water pressure parameter, $\Delta u/\Delta\sigma_1$, at the last step of saturation for 16 undrained tests are summarized in Table 2.

Table 2. Measured $\Delta u/\Delta\sigma_1$ in constant-load tests at the end of saturation stage

Test no.	D_r (%)	σ_v (kPa)	Back pressure (kPa)	σ'_v (kPa)	$\Delta u/\Delta\sigma_1$
9 (B*)	31	175	125	50	0.90
10 (B)	35	175	125	50	0.88
11 (B)	71	205	155	50	0.88
12 (B)	67	205	155	50	0.88
13 (B)	32	275	125	150	0.89
14 (B)	30	275	125	150	0.87
15 (B)	74	305	155	150	0.90
16 (B)	71	305	155	150	0.89
25 (T**)	32	175	125	50	0.91
26 (T)	33	175	125	50	0.90
27 (T)	71	205	155	50	0.88
28 (T)	70	205	155	50	0.85
29 (T)	28	275	125	150	0.86
30 (T)	39	275	125	150	0.91
31 (T)	68	305	155	150	0.82
32 (T)	70	305	155	150	0.83
B*: Babolsar sand, T**: Toyoura sand					

Test Program

Whereas the after consolidation relative density should be taken into account, a series of calibration consolidation tests were conducted to specify the initial relative density of the partially and fully saturated specimens. The values of initial D_r for different vertical σ'_v and post consolidation relative densities as results of preliminary tests are reported in Table 3.

The main experimental program included tests with different values of σ'_v, D_r and γ which were performed under constant-volume and constant-load conditions. Unsaturated samples were sheared under equivalently undrained or constant-volume condition. On the other hand, truly undrained tests were carried out on fully saturated specimens under constant-load condition. Half of the specimens were consolidated to 50 kPa and the others to 150 kPa. Test samples had two different post-consolidation relative densities 30, 70% representing loose and medium dense conditions; respectively. All tests were shear strain-controlled with an approximately sinusoidal shape of cyclic straining at large shear strain amplitudes of 1.0 and 1.5%. The frequency of cyclic loading was 0.5 Hz and the number of loading cycles varied from 1 to 200 or to the cycle of initial liquefaction, which ever occurred first. General testing conditions at the beginning of cyclic shear stage are listed in Table 4 for 32 cyclic simple shear tests.

Table 3. Preliminary tests results

Test no.	Test condition	Post consolidation D_r (%)	σ'_v (kPa)	Initial D_r (%)
P1–B*	Constant-volume	30	50	23.2
P2–B	Constant-volume	70	50	64.9
P3–B	Constant-volume	30	150	16.6
P4–B	Constant-volume	70	150	59.5
P5–B	Constant-load	30	50	3.5
P6–B	Constant-load	70	50	57.9
P7–B	Constant-load	30	150	– 3.7
P8–B	Constant-load	70	150	52.0
P9– T**	Constant-volume	30	50	25.0
P10–T	Constant-volume	70	50	65.7
P11–T	Constant-volume	30	150	20.5
P12–T	Constant-volume	70	150	62.1
P13–T	Constant-load	30	50	4.5
P14–T	Constant-load	70	50	62.7
P15–T	Constant-load	30	150	– 1.7
P16–T	Constant-load	70	150	58.3
B*: Babolsar sand, T**: Toyoura sand				

Table 4. Tests conditions at the beginning of cyclic stage

Test no.	Sand type	Vertical load condition	D_r (%)	γ (%)	σ'_v (kPa)
1, 2	B*	Constant-volume	32, 29	1.0, 1.5	50
3, 4	B	Constant-volume	69, 69	1.0, 1.5	50
5, 6	B	Constant-volume	29, 30	1.0, 1.5	150
7, 8	B	Constant-volume	70, 69	1.0, 1.5	150
9, 10	B	Constant-load	31, 35	1.0, 1.5	50
11, 12	B	Constant-load	71, 67	1.0, 1.5	50
13, 14	B	Constant-load	32, 30	1.0, 1.5	150
15, 16	B	Constant-load	74, 71	1.0, 1.5	150
17, 18	T**	Constant-volume	31, 29	1.0, 1.5	50
19, 20	T	Constant-volume	70, 69	1.0, 1.5	50
21, 22	T	Constant-volume	29, 30	1.0, 1.5	150
23, 24	T	Constant-volume	69, 69	1.0, 1.5	150
25, 26	T	Constant-load	32, 33	1.0, 1.5	50
27, 28	T	Constant-load	71, 70	1.0, 1.5	50
29, 30	T	Constant-load	28, 39	1.0, 1.5	150
31, 32	T	Constant-load	68, 70	1.0, 1.5	150
B*: Babolsar sand, T**: Toyoura sand					

Calculation of G and D

Dynamic stiffness and damping ratio of each cycle can be determined from a graph of stress against strain, knowing as hysteresis loop. Figure 4 illustrates a schematic hysteresis loop and how secant modulus and damping can be determined based on data achieved from stress-strain curve. By using 50 data point per cycle which transferred through CDAS to PC, the area of hysteresis loop can be estimated precisely according to Equation 5.

$$A_{loop} = -0.5\left(\begin{vmatrix}\gamma_1 & \gamma_2\\ \tau_1 & \tau_2\end{vmatrix} + \begin{vmatrix}\gamma_2 & \gamma_3\\ \tau_2 & \tau_3\end{vmatrix} + \cdots + \begin{vmatrix}\gamma_{50} & \gamma_1\\ \tau_{50} & \tau_1\end{vmatrix}\right) \quad (5)$$

in which A_{loop} is the area of hysteresis loop with vertices of (γ_1, τ_1), $(\gamma_2, \tau_2)\ldots(\gamma_{50}, \tau_{50})$ and γ_i, τ_i are shear strain and shear stress at i^{th} point; respectively. Jafarzadeh and Sadeghi 2009

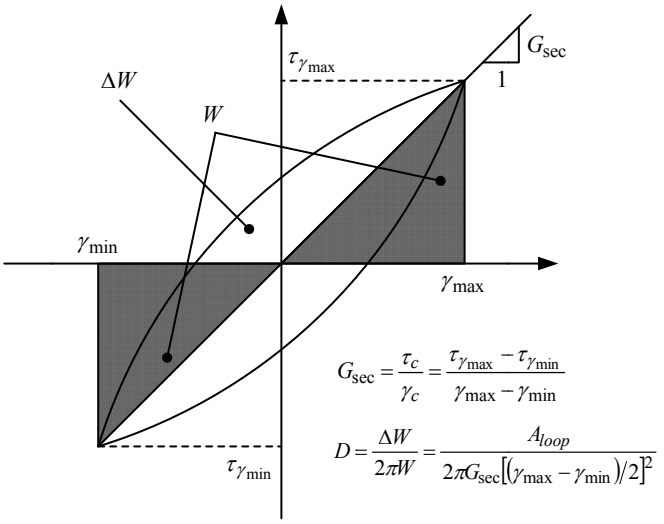

Fig. 4. Estimation of G and D from data of a hysteresis loop.

indicated that the algorithm can also be used in estimation of damping ratio under drained condition.

Typical Test Results

Typical results of constant-load and constant-volume tests are illustrated in Fig. 5. Figure 5a shows the results of a constant-load test (Test #11) conducted on a sample with 70% relative density and 50 kPa vertical effective stress. The shear strain amplitude was 1.0%. Typical results of Test #24 on a medium dense sample with 150 kPa consolidation stress and 1.5% shear strain amplitude under constant-volume condition are also presented in diagrams of Fig. 5b. Figure 5 contains the variations of shear stress, shear modulus and damping ratio with the number of cycles along with the shear stress-strain curves.

RESULTS AND DISCUSSION

Effect of Number of Cycles

Figures 6 and 7 show the variations of shear modulus with the number of cycles for two tested materials. Results of the tests performed under 50 kPa vertical effective consolidation stress represented in Fig. 6 while Fig. 7 includes the data obtained from the other tests with 150 kPa vertical effective stress. Sample specification and testing conditions are also plotted above each chart. These figures compare dynamic stiffness of soil specimens under constant-volume and constant-load conditions. According to the results, shear modulus decreases with the number of cycles under all testing conditions independent of vertical load controlling mode. In the other words, the excess pore water pressure developed due to increase in the number of cycles under constant-load condition as well as constant-volume condition, causes stiffness degradation.

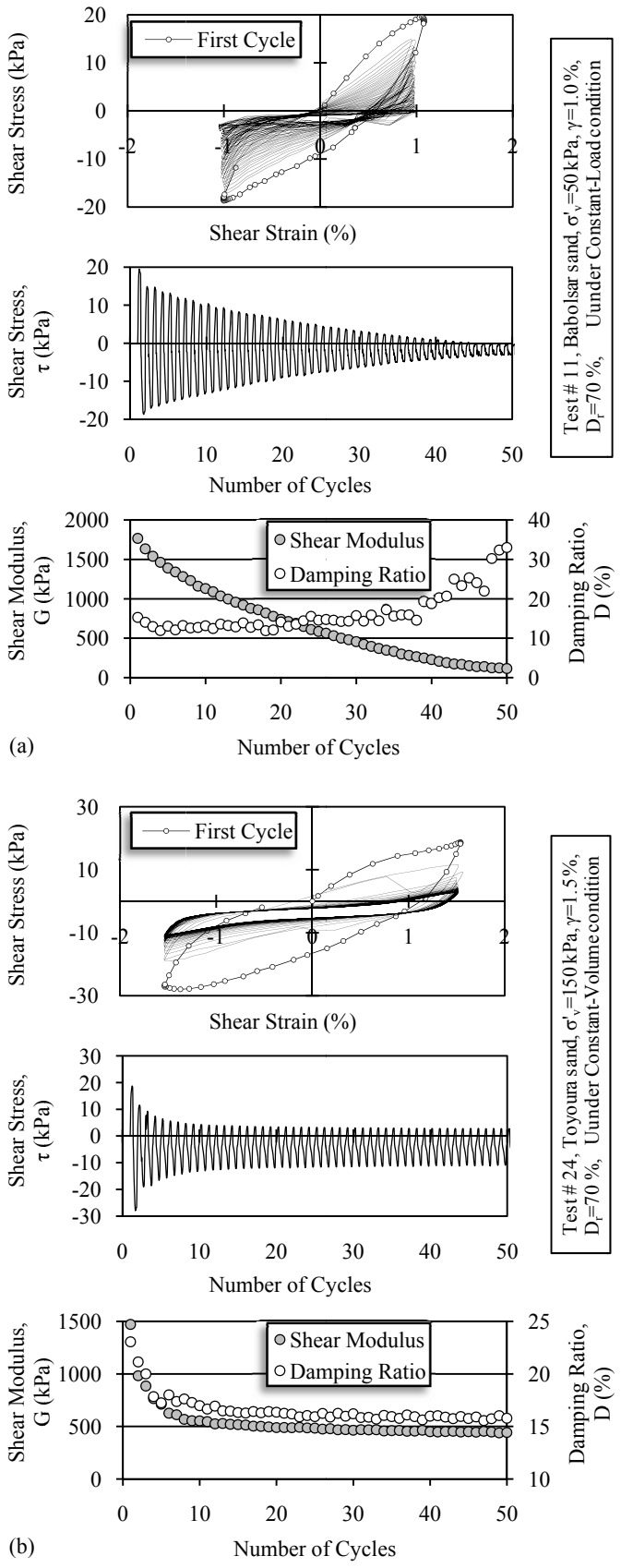

Fig. 5. Typical results of a (a) constant-load test, (b) constant-volume test.

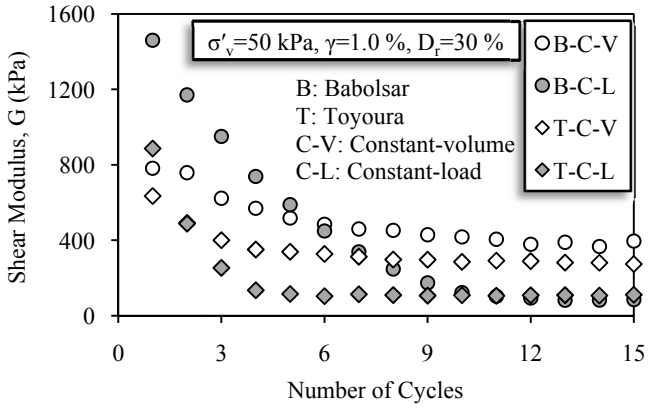

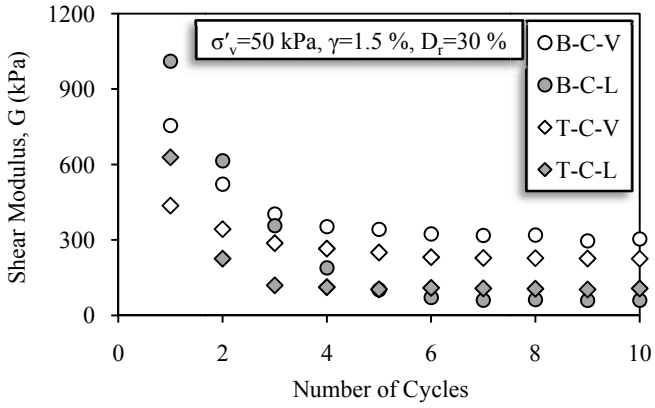

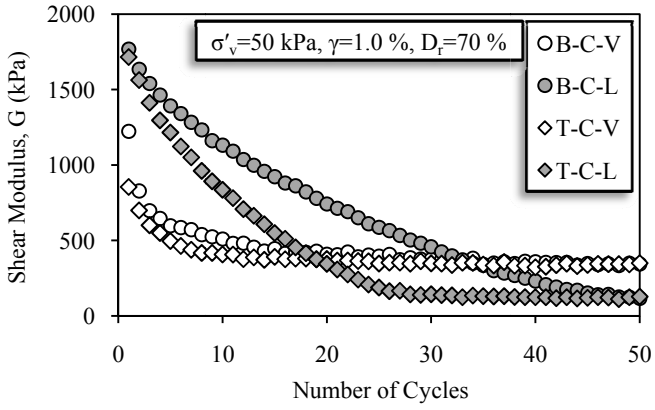

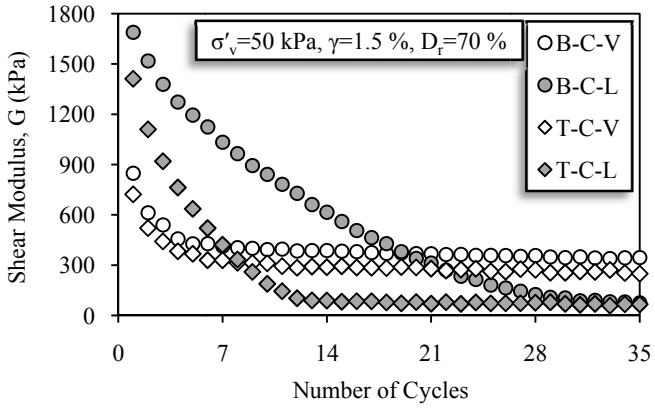

Fig. 6. Variations of shear modulus with the number of cycles for specimens consolidated to 50 kPa vertical effective stress.

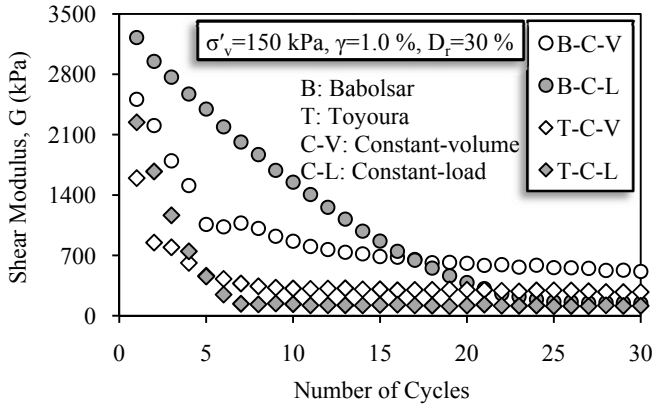

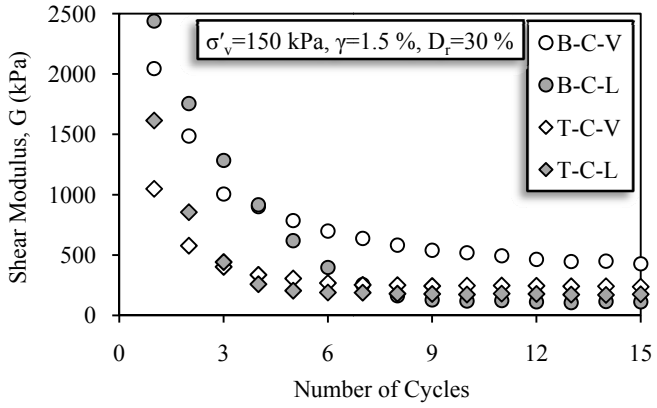

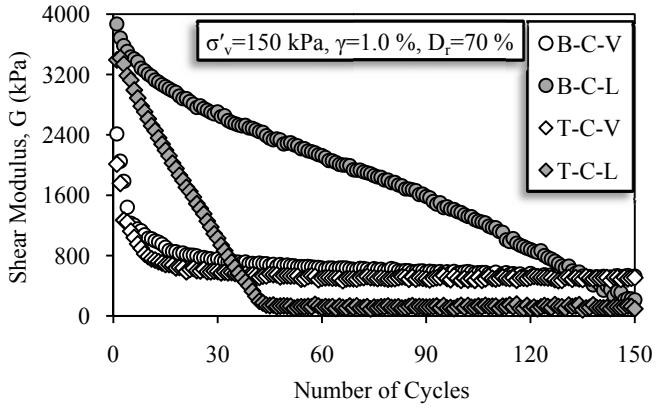

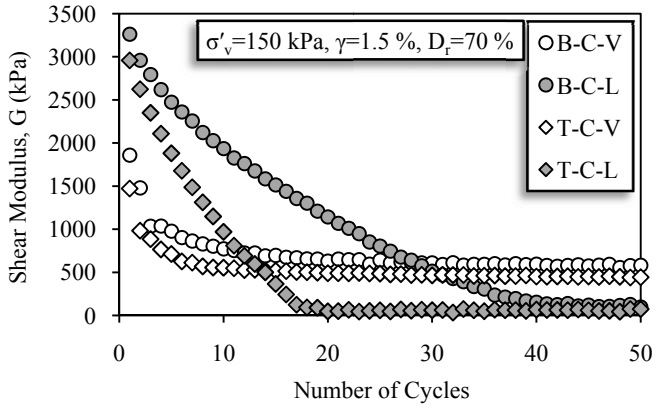

Fig. 7. Variations of shear modulus with the number of cycles for specimens consolidated to 150 kPa vertical effective stress.

The trends of shear modulus variations with the number of cycles are similar under the both truly and equivalently undrained conditions but, the values differ from each other to some extent. The values of shear modulus at cycle 1 for all samples sheared under constant-load condition are more than the corresponding values of constant-volume tests. In addition, in contrast to a specific constant-volume test, lower values of dynamic stiffness are obtained for the corresponding fully saturated sample under constant-load condition after it reaches to the cycle of initial liquefaction and loses its lateral resistance to shear stresses. It means that the range of shear modulus variations with the number of cycles under truly undrained conditions is higher compared to the constant-volume tests while the number of cycles varies between 1 and N_l.

Although both specimens for constant-volume and constant-load tests were prepared by wet tamping and had same relative densities at the beginning of cyclic stage, the specimens sheared under constant-load condition seem to be more homogenous because of the water flushed into the specimens during saturation stage. The water lubricates the surface of grains and makes the movement of grains on each other in desirable directions easier. So it would appear that, the higher value of shear modulus at cycle 1 under constant-load condition compared to the constant-volume tests is because of the more homogenous fabric produced for fully saturated samples than unsaturated samples prepared for constant-volume tests.

As shown previously in Figs. 6 and 7, the values of dynamic stiffness obtained through the constant-load tests are less compared to the results of constant-volume tests after the specimens reach to the initial liquefaction. A possible explanation for the higher values of shear modulus under constant-volume condition may be the residual strength remained in the specimens after liquefaction due to the inter-granular suction forces. Indeed the water content of about 5% which is mixed with dried sand makes the placement of moist sand in a very loose structure possible, because of capillary effects between particles (Ishihara 1996). This amount of water remains in the sample as well as the capillary forces between grains even after the occurrence of imaginary liquefaction. Therefore, constant-volume tests represent more values of shear modulus in contrast to the constant-load tests run on the fully saturated specimens which completely lose their shear strength.

The dependence of damping ratio on the number of cycles under constant-load condition is shown in Fig. 8. Based on the diagrams of Fig. 8 the variations of damping with the number of cycles can be neglected up to 10^{th} cycle before the initial liquefaction. Afterward, damping increases substantially with the number of cycles. It means that for the samples liquefied before 10^{th} cycle, damping values are in ascending order from cycle 1. On the other hand, for samples liquefied after 10 cycles, the number of cycles has a negligible effect on damping variations until 10 cycles to N_l and a significant growth in damping ratio takes place in the last 10 cycles

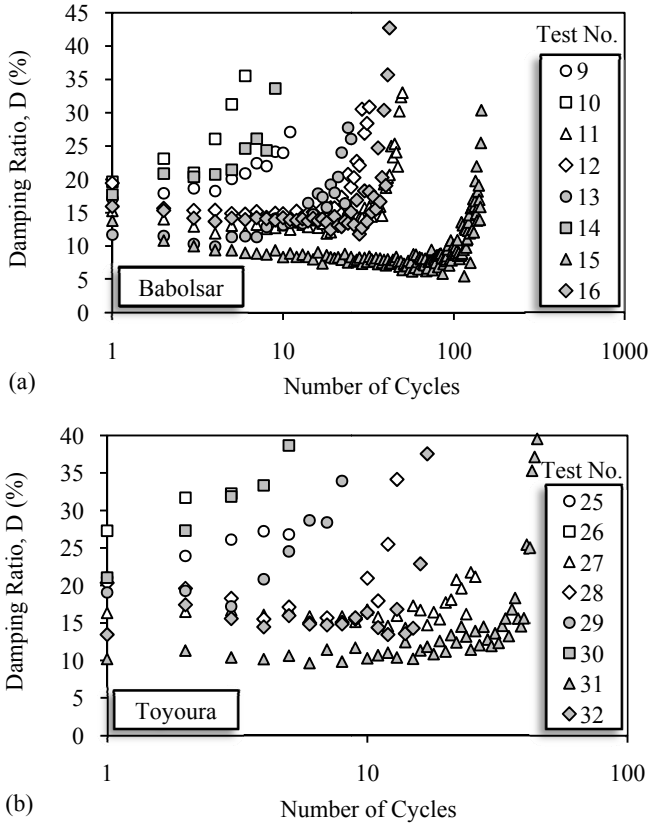

Fig. 8. Variations of damping ratio with the number of cycles for the tests under constant-load condition.

before N_l. Results indicated that, the developed pore water pressure has an important influence on damping variations.

In this study damping values are represented from cycle 1 to N_l. By getting close to the cycle of initial liquefaction, shear strength of a specific sample decreases significantly which results in a significant decrease in shear modulus. Damping increases with a decrease in shear modulus until the occurrence of initial liquefaction, according to Fig. 4. After liquefaction, the horizontal load cell which directly connected to the pneumatic actuator cannot sense the lateral forces precisely. Therefore, the shape of hysteresis loop is miscalculated along with the loop area and shear modulus that subsequently makes damping ratio unreliable. So, it is just assumed that damping values after a sample is liquefied, are the same as damping at N_l.

Figure 9 indicates the variations of damping ratio with the number of cycles for all constant-volume tests. As shown in the diagrams of Fig. 9, damping ratio decreases with the number of cycles. By comparing the results of Figs. 8 and 9, it is inferred that the trends of damping variations with the number of cycles under constant-volume condition are not comparable with those of constant-load tests. In contrast to the constant-load tests, damping will not increase by approaching to the cycle of initial liquefaction under constant-volume condition. It seems that, the tests performed in the present study under constant-load condition represent more reliable

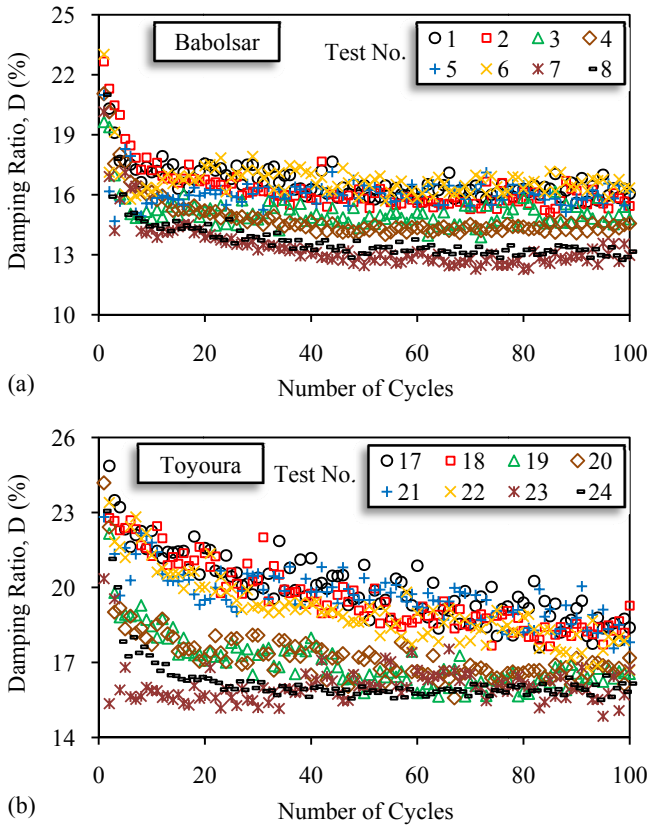

Fig. 9. Variations of damping ratio with the number of cycles for the tests under constant-volume condition.

trends for damping variations with the number of cycles than constant-volume tests.

The main reason for rapid growth in damping ratio with the number of cycles by getting close to the liquefaction state under truly undrained condition was the low shearing resistance of specimens to lateral forces which was correlated with the shear modulus. Subsequently, the lower values of shear modulus result in the higher values of damping ratio (Fig. 4). But, under constant-volume condition the trends of damping variations with the number of cycles are different. Since the specimens were not fully saturated and the developed pore water pressure is imaginary even after the total vertical load was omitted from the specimen, there was an amount of shear modulus which was more in contrast to the truly undrained tests. It means that the specimens had shear strength to the lateral load even after the occurrence of liquefaction due to the capillary effects. This residual value of shear modulus prevents damping from increase as in constant-load tests and keeps it nearly constant with a few scattering until cycle 100.

Effects of D_r, σ'_v and γ

The tests were conducted under two different levels of D_r, σ'_v and γ, while the other testing conditions were kept the same. So, the effects of relative density, vertical effective stress and shear strain amplitude on shear modulus and damping ratio can be investigated under constant-volume and constant-load conditions. Comparisons will be presented and discussed based on the values of shear modulus and damping ratio at cycle 5.

Effect of Relative Density. Figure 10 indicates the effect of relative density on shear modulus and damping ratio of sand. The increase in shear modulus as a result of 40% increase in D_r can be seen in Fig. 10a for constant-volume and constant-load tests. Legends shown at the right side of each diagram contain the numbers of individual tests. Complete test conditions were summarized in Table 5. Conversely, damping ratio descends with an increase in relative density under truly and equivalently undrained conditions as shown in Fig. 10b. The rate of increase in shear modulus due to the growth of relative density from 30 to 70% is more significant for the tests conducted on saturated samples under constant-load condition as well as the rate of reduction in damping ratio. This is because of the effect of excess pore water pressure developed during cyclic shearing and results in stiffness degradation especially for samples with 30% relative density. In the other words, high amount of excess pore water pressure is generated when a specimen is cyclically sheared with the application of large shear strain. This mechanism makes loose samples to lose most of their strength to the lateral forces in the first few cycles, which subsequently results in a substantial decrease in shear modulus along with an increase in damping value. But, as described previously, the values of modulus under constant-volume condition don't reduce with the number of cycles as much as those of constant-load tests because of the capillary effect.

Effect of Vertical Effective Stress. The variations of shear modulus and damping ratio with σ'_v are illustrated in Fig. 11. With an increase in vertical effective stress from 50 to 150 kPa the values of dynamic stiffness significantly increase in both constant-load and constant-volume tests for all testing conditions, based on the results of Fig. 11a. As depicted in Fig. 11b, damping ratio decreases with the increase in vertical effective consolidation stress in all the tests performed under constant-load condition except one, and most of constant-volume tests. Trend of damping variation with σ'_v for two constant-load tests (i.e. 26 and 30) is different from the other tests. These tests had a nominal relative density of 30% and were sheared with 1.5% shear strain amplitude. Both samples liquefied until cycle 5 that means, the values of damping at N_l are not so reliable. However, based on the data depicted in Fig. 8b, the values of damping for the test consolidated to a higher vertical effective stress (test # 30) are less compared with the test # 26 up to third cycle, which is equal to the cycle of initial liquefaction for the test # 26. With regard to the results of constant-volume tests illustrated in Fig. 11b, damping ratio at cycle 5 increases slightly with the increase in σ'_v in two cases of constant-volume tests. The mentioned trend is not expected and also differs from the trend of other cases.

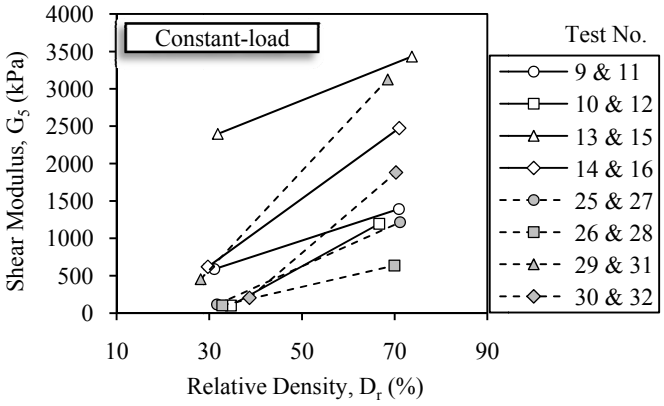

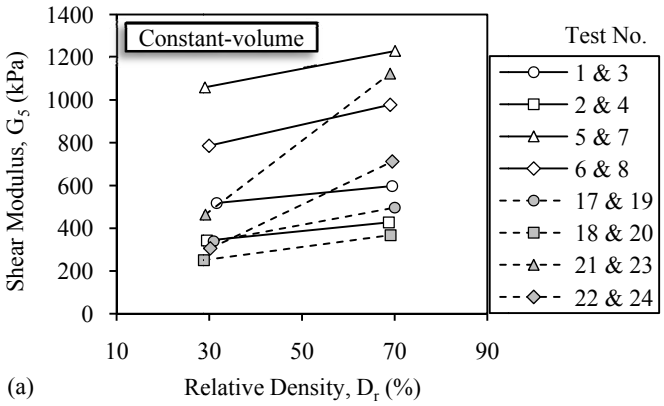

(a)

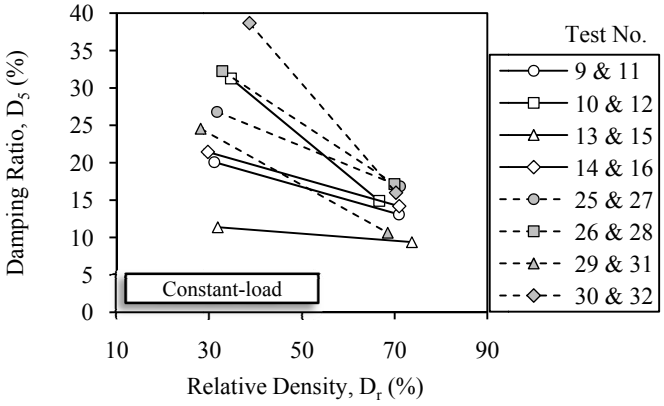

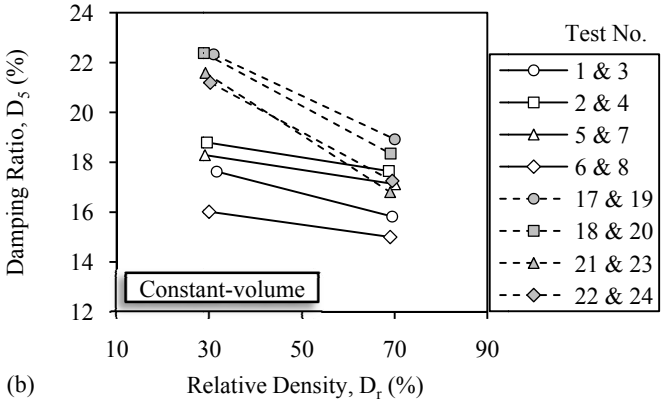

(b)

Fig. 10. Effect of relative density on (a) shear modulus, (b) damping ratio of constant-load and constant-volume tests .

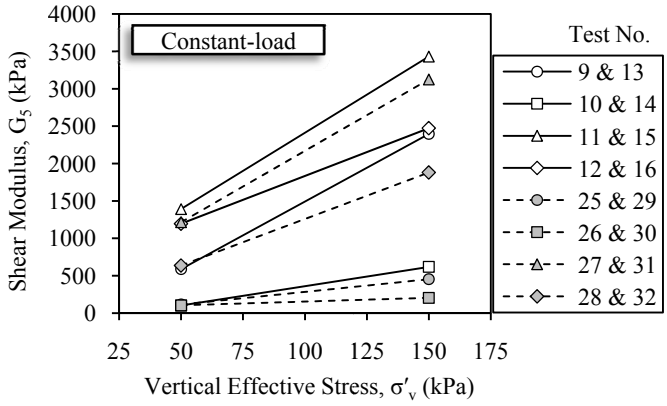

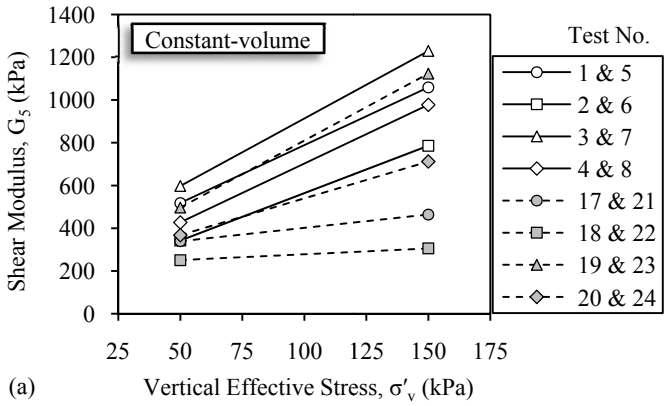

(a)

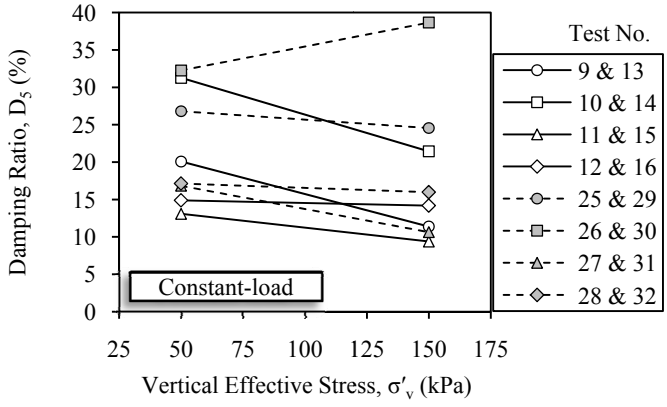

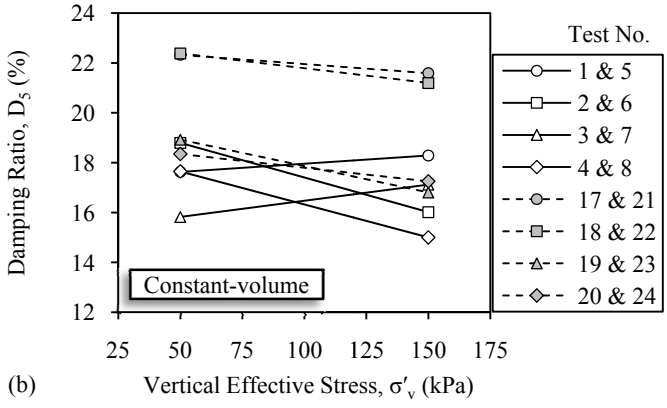

(b)

Fig. 11. Effect of vertical effective stress on (a) shear modulus, (b) damping ratio of constant-load and constant-volume tests .

Effect of Shear Strain Amplitude. The influence of γ on shear modulus and damping ratio of Babolsar and Toyoura sands are demonstrated in Fig. 12. The variations of shear modulus are in descending order with the increase in shear strain amplitude, under constant-volume and constant-load conditions. With 0.5% increase in shear strain amplitude, a significant increase in damping ratio of saturated samples can be seen from the results of truly undrained tests in Fig. 12b. Damping doesn't follow a specific trend in constant-volume tests. In the other words, damping ratio increases slightly with the shear strain amplitude in some cases and the trend is vice versa in the other cases. It seems that, shear strain amplitude has no important effect on damping variation under constant-volume condition.

A statistical study has done in order to compare the effects of D_r, σ'_v and γ on shear modulus and damping ratio of sands tested in the current study under constant-volume and constant-load conditions. Results are shown in the column diagrams in Fig. 13. The average decrease in shear modulus of 2nd, 5th and 10th cycles due to the decrease in D_r and σ'_v and increase in γ is shown in Fig. 13a. Results of constant-load and constant-volume tests are pasted in the upper and lower half of diagram of Fig. 13a; respectively. The average decrease in damping ratio because of the increase in D_r and σ'_v as well as the decrease in γ for truly and equivalently undrained tests is also shown in upper and lower half of Fig. 13b; respectively, for cycles 2, 5 and 10.

Based on the results of Fig. 13a, for example, a decrease in σ'_v from 150 to 50 kPa causes 55% and 60% decrease in G_2 of constant-volume and constant-load tests; respectively. G_5 also decreases by 45% and 65% on average under the mentioned conditions. According to the results of Fig. 13b, 40% reduction in D_r (i.e. 70 to 30%), decreases damping ratio of constant-volume and constant-load tests at cycle 2 by 11% and 29% on average; respectively. Also, the average decrease in damping ratio at cycle 5 due to the reduction in D_r grows to 13% and 42%; respectively, for constant-volume and constant-load tests. Therefore, the column charts indicated in Fig. 13 can be used to moderately specify how much a certain parameter affects shear modulus and damping ratio of similar materials under different loading conditions.

Of particular interest was a comparison between constant-volume and constant-load conditions on test results. If the influences of D_r, σ'_v and γ on shear modulus and damping ratio of tested sands under constant-volume and constant-load conditions were completely the same, the horizontal axis in the column charts of Fig. 13 would act like a mirror. Actually, D_r, σ'_v and γ have similar effects on trends of shear modulus variations under both constant-volume and constant-load conditions, but the quantities are somewhat different. D_r and σ'_v also affect damping ratio in similar way with different magnitudes under both conditions but, it seems that damping ratio is not affected by shear strain amplitude under constant-volume compared with constant-load condition.

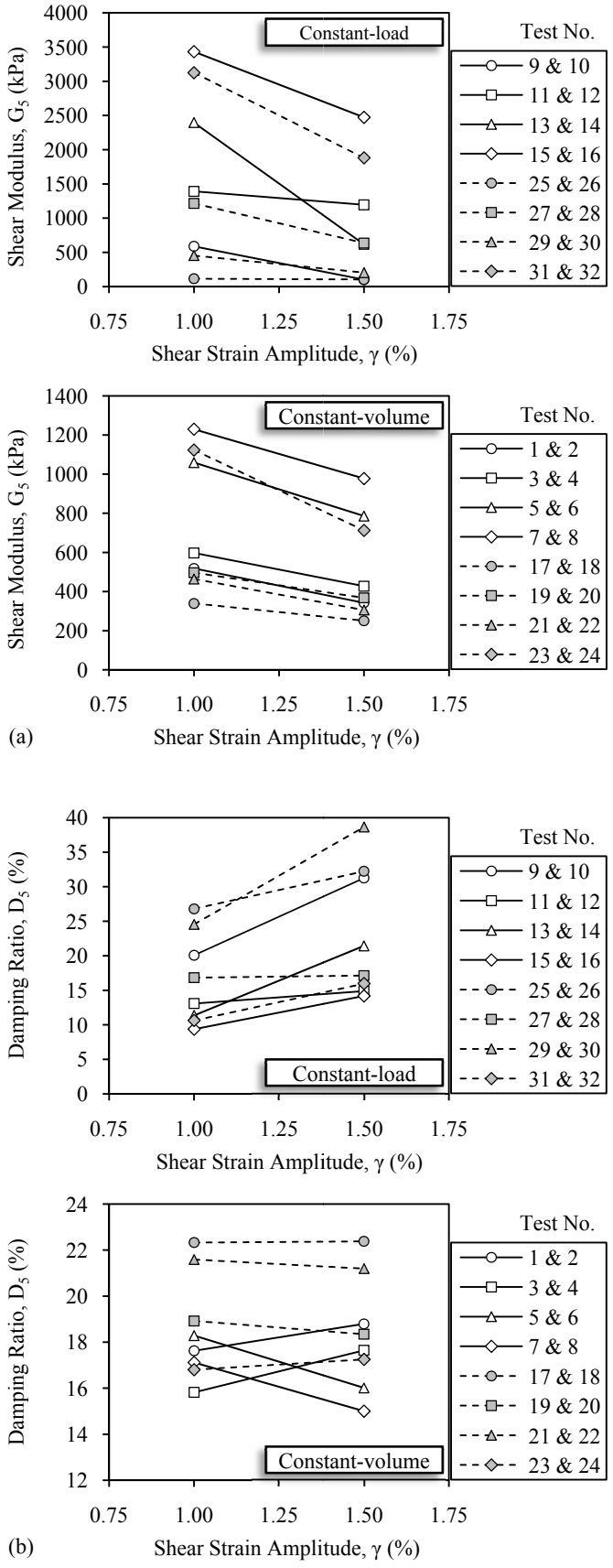

Fig. 12. Effect of shear strain amplitude on (a) shear modulus, (b) damping ratio of constant-load and constant-volume tests .

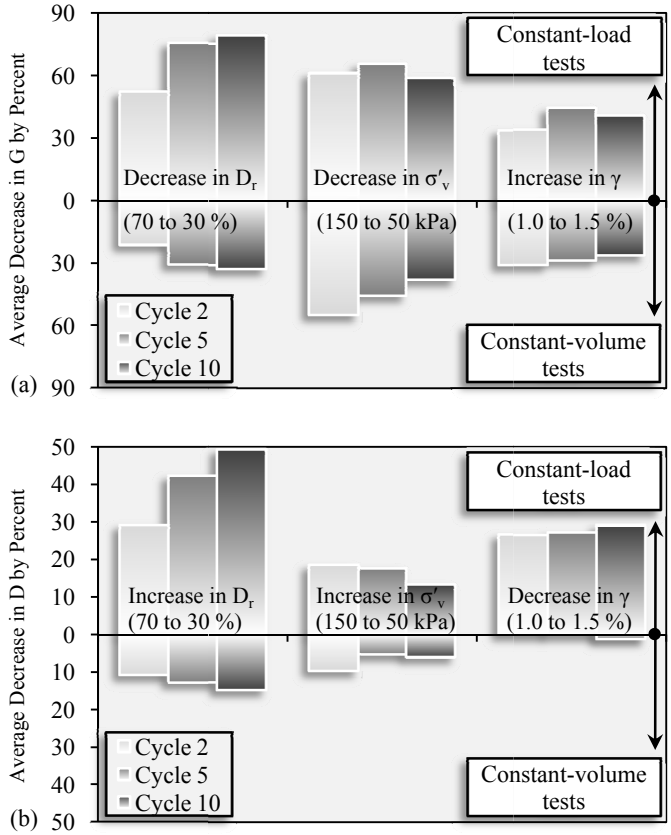

Fig. 13. Effects of D_r, σ'_v and γ on (a) shear modulus and (b) damping ratio in constant-load and constant-volume tests.

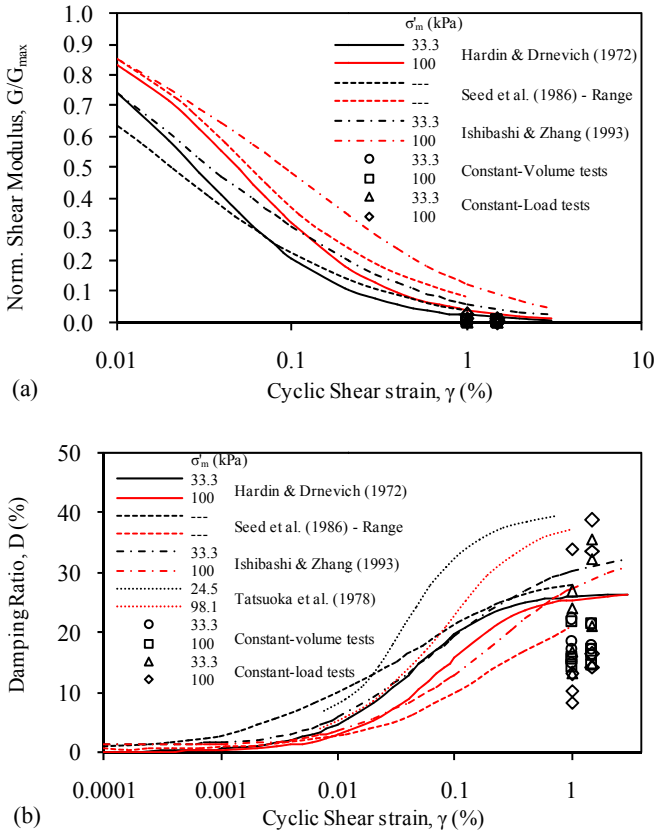

Fig. 14. Comparison of measured (a) G/G_{max}-γ and (b) D-γ with the previously published curves of other investigators.

Based on the results of Fig. 13, it is revealed that, the effects of D_r, σ'_v and γ on variations of shear modulus and damping ratio are more pronounced under constant-load condition. Some of possible explanations for differences observed under both conditions are the different fabric of unsaturated and saturated testing samples, the capillary effects in samples prepared for constant-volume tests and the real pore water pressure developed under constant-load condition. The mentioned reasons were discussed previously in detail.

Shear modulus and damping ratio of two tested sands

Data of shear modulus and damping ratio of Babolsar sand were compared with the corresponding values for Toyoura sand. Higher values of shear modulus as well as lower values for damping were observed for Babolsar sand compared to Toyoura sand during cyclic simple shear tests performed in the current study. According to the results, shear modulus of Toyoura sand is approximately 30% less than Babolsar sand. Damping ratio of Toyoura sand is also more than damping of Babolsar sand by nearly 20% on average.

Figure 14 compares the measured normalized shear modulus and damping ratio in this study with the previously published curves of other investigators. Values of G_{max} were estimated on the basis of Equation 6 suggested by Kokusho 1980.

$$G_{max} = 8400(2.17 - e)^2 \times (\sigma'_m)^{0.5}/(1 + e) \quad \text{(kPa)} \quad (6)$$

where σ'_m and e are mean principal effective stress and void ratio; respectively. As shown in Fig. 14a, data obtained through cyclic simple shear tests follow the curves of Hardin and Drnevich 1972b as well as the lower bound of Seed et al. 1986 for sands. Comparison of damping ratio measured in constant-volume and constant-load tests with the proposed curves by other researchers in Fig. 14b reveals that, although there is not a good agreement between data obtained in this study, but the differences between reported curves of others for damping ratio of sand at large shear strain amplitude are also tremendous. However, some of damping values measured in the current study fall between the lower bound of Seed et al. 1986 and curve of Tatsuoka et al. 1978 for a mean principal effective stress equals to 24.5 kPa.

CONCLUSIONS

A SGI cyclic simple shear apparatus was instrumented with a pressure test device in order to modify the conventional device, so it can be used in conducting tests on fully saturated specimens. This method of saturation yields reliable results by performing real undrained tests. Testing program included 32 constant-volume and constant-load tests on partially and fully saturated specimens; respectively, under different conditions.

The following can be drawn on the basis of the current experimental study.

An increase in D_r and σ'_v as well as a decrease in γ, result in a growth in shear modulus along with a reduction in damping ratio under constant-load condition. These parameters have similar effects on shear modulus and damping ratio under constant-volume condition except the shear strain amplitude which has no significant effect on damping ratio. Trends of shear modulus variations with the number of cycles are in descending order under both conditions. Damping didn't widely vary with the number of cycles until 10 cycles to N_l under constant-load condition and afterward a significant growth in damping values were observed. Conversely, damping ratio of constant-volume tests decreases with the number of cycles and the trend is complicated to be judged.

Comparisons between the results of constant-volume and constant-load tests reveal that, shear modulus and damping ratio are much affected by D_r, σ'_v, γ and the number of cycles under constant-load condition. It is found that some differences exist between two kinds of samples prepared for tests which should be taken into account. First, saturated samples are more homogenous than unsaturated samples. Second, capillary forces affect the response of constant-volume test samples during the whole cyclic stage whereas such effects do not exist in saturated specimens. So, it would appear that observed differences between the results of constant-volume and constant-load tests may be because of the different fabric produced in saturated and unsaturated samples rather than of the vertical load controlling mode. However, further work is needed to compare the results of constant-volume tests on completely dry and saturated sand with constant-load test results on saturated sand.

REFERENCES

Das, B.M. [1983]. "*Advanced Soil Mechanics*". Chapter 4. Hemisphere Publishing, New York.

Dyvik, R., T. Berre, S. Lacasse and B. Raadim [1978], "Comparison of Truly and Constant Volume Direct Simple Shear Tests", Geotechnique., Vol. 37(1), pp. 3-10.

Hardin, B.O., V.P. Drnervich [1972a], "Shear Modulus and Damping in Soils: measurement and parameter effects", J Soil Mech Found Div, ASCE Vol. 98(6), pp. 603-624.

Hardin, B.O., V.P. Drnervich [1972b], "Shear Modulus and Damping in Soils: Design Equations and Curves", J Soil Mech Found Div, ASCE Vol. 98(7), pp. 667-692.

Head K.H. [1998]. "*Manual of Soil Laboratory Testing*". 2nd Edition, Vol. 3, Chapter 15. John Wiley & Sons, New York.

Ishibashi, I. and X. Zhang [1993], "Unified Dynamic Shear Moduli and Damping Ratios of Sand and Clay", Soils Found Vol. 33(1), pp. 182-191.

Ishihara K. [1996]. "*Soil Behavior in Earthquake Geotechnics*". Oxford University Press, Great Britain.

Jafarzadeh, F., and H. Sadeghi [2009], "Effect of Water Content on Dynamic Properties of Sand in Cyclic Simple Shear Tests", *Proc. Intern. Conf. on Performance-Based Design in Erthq. Geotech Engrg. (IS-Tokyo 2009)*, pp. 1483-1490.

Kokusho, T. [1980], "Cyclic Triaxial Test of Dynamic Soil Properties for Wide Strain Range", Soils Found Vol. 20(2), pp. 45-60.

Kramer SL. [1996]. "*Geotechnical Earthquake Engineering*". Chapter 6. Prentice Hall, Upper Saddle River.

Seed, H.B., R.T. Wong, I.M. Idriss and K. Tokimatsu [1986], "Moduli and Damping Factors for Dynamic Analysis of Cohesionless Soils", J Geotech Eng Vol. 112(11), pp. 1016-1032.

Tatsuoka, F., T. Iwasaki and Y. Takagi [1978], "Hysteretic Damping of Sands under Cyclic Loading and Its Relation to Shear Modulus", Soils Found Vol. 18(2), pp. 25-40.

Vanden Berghe, J.F., A. Holeyman and R. Dyvik [2001], "Comparison and Modeling of Sand Behavior under Cyclic Direct Simple Shear and Cyclic Triaxial Testing", *Proc. Fourth Intern. Conf. on Recent adv. in Geo. Erthq. Engrg. and Soil Dyn.*, Paper No. 1.52.